Controlled Vortex-Sound Interactions in Atomic Bose-Einstein Condensates

N. G. Parker,[1] N. P. Proukakis,[1] C. F. Barenghi,[2] and C. S. Adams[1]
[1]*Department of Physics, University of Durham, South Road, Durham DH1 3LE, United Kingdom*
[2]*School of Mathematics and Statistics, University of Newcastle, Newcastle upon Tyne, NE1 7RU, United Kingdom*
(Received 19 December 2003; published 20 April 2004)

The low temperature dynamics of a vortex in a trapped quasi-two-dimensional Bose-Einstein condensate are studied quantitatively. Precession of an off-centered vortex in a dimple trap, embedded in a weaker harmonic trap, leads to the emission of sound in a dipolar radiation pattern. Sound emission and reabsorption can be controlled by varying the depth of the dimple. In a shallow dimple, the power emitted is proportional to the vortex acceleration-squared over the precession frequency, whereas for a deep dimple, periodic sound reabsorption stabilizes the vortex against radiation-induced decay.

DOI: 10.1103/PhysRevLett.92.160403 PACS numbers: 03.75.Lm, 47.32.Cc, 67.40.Vs

The superfluid nature of weakly interacting atomic Bose-Einstein condensates (BECs) supports quantized circulation, as observed in the form of single vortices [1], vortex lattices [2], and vortex rings [3]. Vortices are fundamental to the understanding of fluid dynamics, signaling the breakdown of ordered flow and the onset of turbulence. Dilute atomic gases enable easy control and observation of quantized vortices, complimenting vortex studies in liquid helium, superconductors, and nonlinear optics. Vortices in superfluids are subject to both thermal and dynamical instabilities. Thermal dissipation in BECs induces an outward motion of the vortex towards lower densities [4]. Dynamical dissipation is evident in superfluids in the limit of low temperature, as manifested in the temperature-independent crystallization of vortex lattices in BECs [5], and the decay of vortex tangles in liquid helium [6]. In this limit, reconnections and Kelvin wave excitations of vortex lines lead to dissipation by sound (phonon) emission [7,8]. Superfluid vortices are also unstable to acceleration, in analogy to Larmor radiation induced in accelerating charges. For example, corotating pairs [9], and single vortices performing circular motion [7,10], within a two-dimensional (2D) homogeneous superfluid are predicted to decay via sound emission. However, this decay mechanism is not expected to occur in finite-sized BECs due to the sound wavelength being larger than the system size [10,11].

In this Letter we show that a vortex in a trapped quasi-2D BEC, precessing due to the inhomogeneous background density, emits dipolar sound waves in a spiral wave pattern. The quasi-2D geometry ensures that the vortex line is effectively rectilinear and that Kelvin wave excitations [12,13] are negligible. This instability is closely analogous to the decay of dark solitons in quasi-1D BECs via sound emission due to longitudinal confinement [14,15]. Quasi-2D "pancake" BECs have recently been created experimentally, using tight confinement in one dimension [16,17]. Although such systems are prone to strong phase fluctuations, these effects are suppressed in the limit of very low temperature [18,19]. In a harmonic trap sound reabsorption occurs, stabilizing the vortex (in the absence of other decay mechanisms), while, in modified trap geometries, sound reabsorption can be prevented for times long enough to enable the vortex decay to be observed and probed. In the latter case, the power radiated by the vortex is found to be proportional to the vortex acceleration squared and inversely proportional to the precession frequency.

Our analysis is based on the Gross-Pitaevskii equation (GPE) describing the mean-field dynamics of a weakly interacting BEC in the limit of low temperature,

$$i\hbar\frac{\partial\psi}{\partial t} = -\frac{\hbar^2}{2m}\nabla^2\psi + V_{\rm ext}\psi + g|\psi|^2\psi - \mu\psi. \quad (1)$$

Here ψ is the macroscopic order parameter of the system, m is the atomic mass, and $\mu = ng$ is the chemical potential, where n is the atomic density. The atomic scattering amplitude $g = 4\pi\hbar^2 a/m$, where a is the s-wave scattering length, is taken to be positive, i.e., repulsive interatomic interactions. The external confining potential $V_{\rm ext}$ is given by

$$V_{\rm ext} = V_0\left[1 - \exp\left(-\frac{2r^2}{w_0^2}\right)\right] + \frac{1}{2}m\omega_r^2 r^2 + \frac{1}{2}m\omega_z^2 z^2 \quad (2)$$

and consists of a Gaussian dimple with waist w_0 and depth V_0 embedded within a weaker harmonic trap. This configuration can be realized experimentally by focussing a far-off-resonant red-detuned laser beam in the center of a magnetic trap. Close to the center, the Gaussian dimple is approximately harmonic with frequency $\omega_d = 2\sqrt{V_0}/w_0$. For trap parameters, $\omega_r = 2\pi \times 5$ Hz, $\omega_d = 20\omega_r$, and $\omega_z = 200\omega_r$ (we choose $\omega_z \gg \omega_r$ to suppress excitation in the z direction), the harmonic oscillator time is $\omega_d^{-1} =$ 1.6 ms. In this case, the time scale of dynamical instability due to sound emission is much shorter than the expected thermodynamic vortex lifetime, which is of the order of seconds [4]. Assuming a peak density $n_0 = 10^{14}$ cm^{-3} and a chemical potential $\mu = 3.5\hbar\omega_d$, a ^{87}Rb (^{23}Na) BEC has the harmonic oscillator length

 0031-9007/04/92(16)/160403(4)$22.50

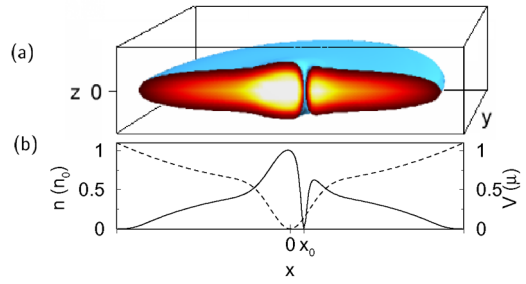

FIG. 1 (color online). (a) Isosurface plot of the atomic density ($n = 0.1n_0$, where n_0 is the peak density) of a quasi-2D BEC, confined by the potential of Eq. (2), with a vortex at $(x_0, 0)$. In the x-z plane ($y = 0$), white and black corresponds to high and low density, respectively. (b) Density (solid line) and potential (dashed line) along the x direction ($y = 0, z = 0$).

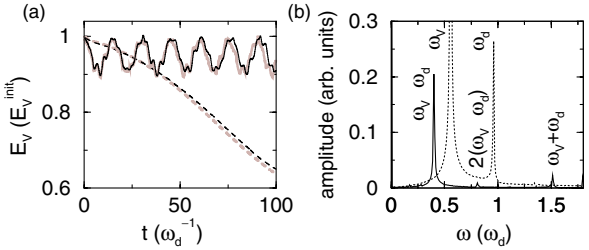

FIG. 2 (color online). (a) 3D (black) and 2D (grey) energy of an off-centered vortex, initially located at $(0.53, 0)l_d$, rescaled by the initial vortex energy. $V_0 = 10\mu$ (solid lines): sound reabsorbed. $V_0 = 0.6\mu$, $\omega_r = 0$ (dashed lines): sound escapes. (b) Fourier spectrum of the vortex x coordinate (dotted line) and energy (solid line) for $V_0 = 10\mu$, using the 2D GPE.

$l_d = \sqrt{\hbar/(m\omega_d)} = 1.1(2.1)\ \mu$m and the healing length $\xi = \hbar/\sqrt{m\mu} = 0.53 l_d$.

A singly quantized vortex, initially at position (x_0, y_0) in the dimple (illustrated in Fig. 1), is expected to precess around the trap center, along a path of constant potential, as observed experimentally [20]. This can be interpreted in terms of the Magnus force induced by the density gradient [21,22]. However, the acceleration of the vortex produces sound emission. By varying the depth of the dimple, we show how this emission can be observed and quantified. Analogous control has previously been demonstrated for dark solitons [15].

The energy of a precessing vortex, for both deep $V_0 \gg \mu$ and shallow $V_0 < \mu$ dimples, is shown in Fig. 2(a). The vortex energy is monitored by integrating the GP energy functional,

$$E = -\frac{\hbar^2}{2m}|\nabla\psi|^2 + V_{\rm ext}\psi^2 + \frac{g}{2}|\psi|^4, \qquad (3)$$

across a "vortex region," defined to be a circle of radius 5ξ centered on the core, and subtracting off the corresponding contribution of the background fluid. Although the vortex energy technically extends up to the boundary of the system, this region contains ~50% of the total vortex energy at all background densities considered here.

For $\omega_z \gg \omega_r$ and providing $l_z \gg a$, where l_z is the transverse harmonic oscillator length, the GPE can be reduced to a 2D form with a modified coefficient $g_{2D} = g/(\sqrt{2\pi} l_z)$ [18,23]. In Fig. 2(a) we compare the full 3D GPE (black lines) with the computationally less demanding 2D GPE (grey lines), where the 2D and 3D density profiles are matched as closely as possible. The excellent agreement justifies the use of the 2D GPE for subsequent results.

For a deep dimple, the emitted sound waves are confined to the dimple region and reinteract with the vortex, and there is no *net* decay of the vortex energy. The energy oscillations [solid lines in Fig. 2(a)] correspond to a beating between the vortex mode and the collective excitations of the trapped condensate. The beating effect is illustrated in Fig. 2(b), where we plot the Fourier transform of the vortex x coordinate (dotted line) and energy (solid line). The two fundamental frequencies, the effective trap frequency ω_d and vortex precession frequency ω_v, dominate the position spectrum, while the energy spectrum highlights the beat frequencies, $(\omega_v - \omega_d)$, $(\omega_v + \omega_d)$, and higher order combinations. Similar beating effects are observed for a driven vortex [24], and between a dark soliton and the dipole mode in a quasi-1D BEC [15]. In contrast, for a shallow dimple, $V_0 < \mu$, the radiated sound escapes, and the vortex energy decays monotonically [dashed lines in Fig. 2(a)].

In an experiment, the vortex energy can be extracted by measuring its position. The trajectory of the vortex for both deep (solid line) and shallow (dashed line) dimples is shown in Fig. 3. For $V_0 \gg \mu$, the orbit is essentially closed, with the vortex remaining in the effectively harmonic region of the dimple, but features a small modulation due to the interaction with the collective excitations of the background fluid. In stark contrast, for

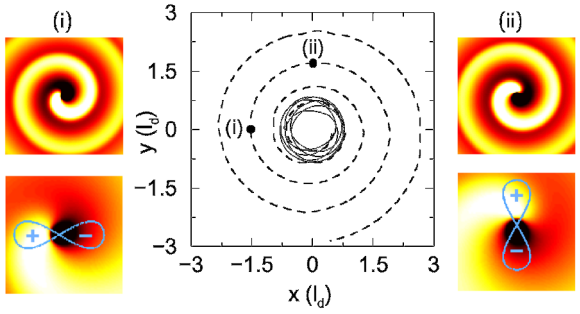

FIG. 3 (color online). Path of a vortex initially at $(0.53, 0)l_d$. $V_0 = 10\mu$ (solid line): mean radius is constant, but modulated by the sound field. $V_0 = 0.6\mu$, $\omega_r = 0$ (dashed line): vortex spirals outwards. Insets: Carpet plots of renormalized density (actual minus background density) for $V_0 = 0.6\mu$ at times (i) $t = 61.4$ and (ii) $t = 63.3\ \omega_d^{-1}$, showing the emission of positive (white) and negative (black) sound waves of amplitude $\sim 0.01 n_0$. Top: Far field $[-50, 50] \times [-50, 50]$. Bottom: Near field $[-14, 14] \times [-14, 14]$, with schematic illustration of dipolar radiation pattern.

$V_0 < \mu$, the vortex spirals out to lower densities. A similar outward motion has recently been predicted for a vortex precessing in a harmonic trap modulated by an optical lattice [25]. The results presented here are for a homogeneous outer region $\omega_r = 0$. Simulations for $\omega_r \neq 0$ are essentially indistinguishable up to a time when the sound reflects off the condensate edge and returns to the dimple. For example, for an outer trap $\omega_r = \omega_d/20$, the emitted sound begins to reinteract with the vortex at $t \sim 80\omega_d$. Following this interaction with the reflected sound, the vortex decay is slowed down, but not fully stabilized, due to a dephasing of the sound modes in the outer trap. Weakly anisotropic 2D geometries yield the same qualitative results, with vortex precession now occurring in an ellipse rather than a circle. In the limit of strong anisotropy, deviations arise as the system tends towards the quasi-1D regime, where vortices are not supported.

The continuous emission of sound waves during the precessional motion is evident by a close inspection of the surrounding density distribution during the course of the decay (insets of Fig. 3). The waves are emitted perpendicularly to the instantaneous direction of motion in the form of a dipolar radiation pattern, while the spiralling motion of the vortex modifies this into a dramatic swirling radiation distribution, reminiscent of spiral waves often encountered elsewhere in nature [26]. The wavelength of the emitted sound $\lambda \sim 25 l_d$ agrees well with the theoretical prediction of $\lambda \sim 2\pi c/\omega_v = 21.3 l_d$ [11], where $c = \sqrt{\mu/m}$ is the speed of sound and ω_v is the vortex precession frequency.

The power radiated by the vortex, in the limit of no reinteraction with the emitted sound ($V_0 = 0.6\mu$), is shown in Fig. 4 as a function of time and radius from the trap center. Because of constraints on the size of our computational grid, this plot was mapped out by a few simulations, with the vortex being started progressively further from the trap center. This could also be implemented experimentally in order to trace out the vortex decay. The curve can be understood qualitatively by considering the density inhomogeneity that the spiraling vortex experiences: the emitted power increases in line with the local radial density gradient up to $r \approx 1.4\xi$, where the gradient of the Gaussian potential is a maximum, and subsequently tails off as the trap gradient decreases smoothly to zero. We have additionally considered the case where the dimple is harmonic instead of Gaussian, and find the same qualitative results, but with enhanced power emission for a particular ω_d due to the larger precession frequency (see inset of Fig. 5). In a harmonic trap of frequency ω, the vortex precession frequency is predicted to be $\omega_v = (3\hbar\omega^2/4\mu)\ln(R/\xi)$, where $R = \sqrt{2\mu/m\omega^2}$ is the Thomas-Fermi radius of the BEC [22]. For a harmonic trap with a cutoff ($V = V_0$ for $r > r_0$), the vortex frequency (inset of Fig. 5, crosses) agrees well with this prediction. However, for a Gaussian dimple of depth V_0, ω_v falls short of this prediction due to the tailing off of the Gaussian potential with radius, as shown in Fig. 5 (inset, circles).

A 2D homogeneous superfluid can be mapped on to a (2 + 1)D electrodynamic system, with vortices and phonons playing the role of charges and photons, respectively [27]. By analogy to the Larmor radiation for an accelerating charge and the power emitted from an accelerating dark soliton in a quasi-1D BEC [15], we assume the power radiated P by the spiralling vortex to be proportional to the square of the local vortex acceleration a. The coefficient of this relation, P/a^2, has been mapped out over a range of dimple strengths, as shown in Fig. 5. Each data point corresponds to the best-fit power coefficient and the average vortex precession frequency for that simulation. Note that there are limitations to the range of precession frequencies that we can probe, just as would be experienced experimentally: in the limit of very tight dimples, the vortex escapes almost instantaneously,

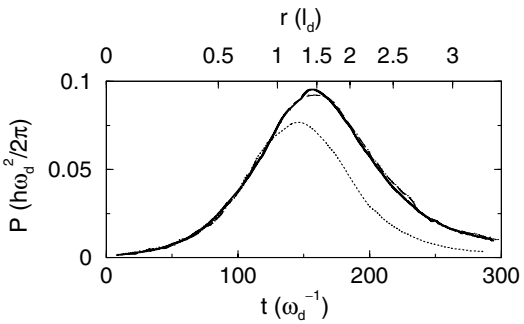

FIG. 4. Power radiated as a function of radius from the trap center (top axis) and time (bottom axis), as calculated from the GP energy functional (solid line). Equation (4) with $\beta = 6.1$ (dashed line). Acceleration-squared law with constant coefficient $26.6(m/\omega_d)$ (dotted line).

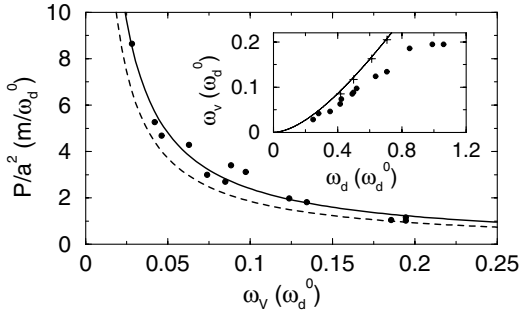

FIG. 5. Coefficient of an acceleration squared power law, P/a^2, for a vortex, calculated over a variety of trap strengths ω_d, as a function of ω_v (circles), along with the analytical predictions [7,10] (dashed line), and best fit line corresponding to Eq. (4) with $\beta = 6.3 \pm 0.86$ (solid line). Here frequency is scaled in terms of ω_d^0, defined by $\mu = 3.5\hbar\omega_d^0$. (The gradient of the best fit line in log-log plot is found to be -1.04.) Inset: Variation of ω_v with trap strength for a Gaussian dimple (circles) and harmonic trap with a cutoff (crosses), along with the theoretical prediction [22] (solid line, see text).

whereas for very weak dimples, the vortex motion is too slow for such effects to be systematically studied. The data indicates a strong dependence on the inverse of the ω_v, suggesting a modified power law of the form

$$P = \beta m n_0 \xi^2 \frac{a^2}{\omega_v}, \tag{4}$$

where β is a dimensionless coefficient. An equation of this form for circular vortex motion in a homogeneous 2D fluid has been obtained by Vinen [7] using classical acoustics and by Lundh and Ao [10] by mapping the superfluid hydrodynamic equations onto Maxwell's electrodynamic equations. Both approaches predict a rate of sound emission proportional to $\omega_v^3 r_v^2$, where r_v is the precession radius, and yield a coefficient $\beta = \pi^2/2$. Despite the assumptions of perfect circular motion, a point vortex, and an infinite homogeneous system, there is remarkable agreement with our findings which indicate $\beta \sim 6.3 \pm 0.9$ (1 standard deviation), with the variation due to a weak dependence on the geometry of the system. We believe that the deviation from the predicted coefficient arises primarily due to the radial component of the vortex motion, which is ignored in the analytical derivations.

Also plotted in Fig. 4, alongside the power emission from the GP energy functional, are an acceleration-squared law (dotted line) and the modified acceleration-squared law of Eq. (4) (dashed line), with the coefficients being chosen to give a best fit. Both lines give excellent agreement until the vortex starts to escape the dimple region at $r \sim 1.4 l_d$. Here the vortex frequency, which previously remained roughly constant, starts to decrease due to the form of the local density. This causes the acceleration-squared law to deviate significantly, while the $1/\omega_v$ term in Eq. (4) corrects for this deviation, giving excellent agreement throughout the decay.

Sound radiation due to acceleration may be important in the case of turbulent vortex tangles in liquid helium, where evidence suggests that the vortex line length L (providing a measure of the energy of the system) decays at a rate proportional to L^2 [7]. In the limit of low temperature, this decay is believed to be primarily due to reconnections and Kelvin wave excitations. We note that, for a system of many vortices, where the acceleration is induced by the surrounding vortex distribution, Eq. (4) would also lead to an L^2 decay.

In summary, we have shown that a vortex precessing in a trapped quasi-2D BEC at low temperature emits dipolar radiation, which becomes modified into a spiral wave pattern due to the motion of the vortex. The vortex energy decays at a rate proportional to its acceleration squared and inversely proportional to the precession frequency. For appropriate trap geometries, the sound emission is experimentally observable via the spiraling motion of the vortex towards lower densities. An analogous instability may arise in the case of optical vortices, which also exhibit a fluidlike motion [28]. For harmonic traps the vortex decay is stabilized by reinteraction with the emitted sound.

We acknowledge financial support from the UK EPSRC.

[1] M. R. Matthews *et al.*, Phys. Rev. Lett. **83**, 2498 (1999).
[2] J. R. Abo-Shaeer, C. Raman, J. M. Vogels, and W. Ketterle, Science **292**, 476 (2001).
[3] B. P. Anderson *et al.*, Phys. Rev. Lett. **86**, 2926 (2001).
[4] P. O. Fedichev and G. V. Shlyapnikov, Phys. Rev. A **60**, R1779 (1999).
[5] J. R. Abo-Shaeer *et al.*, Phys. Rev. Lett. **88**, 070409 (2002).
[6] S. L. Davis *et al.*, Physica (Amsterdam) **280B**, 43 (2000).
[7] W. F. Vinen, Phys. Rev. B **61**, 1410 (2000); W. F. Vinen, Phys. Rev. B **64**, 134520 (2001).
[8] M. Leadbeater *et al.*, Phys. Rev. Lett. **86**, 1410 (2001); M. Leadbeater, D. C. Samuels, C. F. Barenghi, and C. S. Adams, Phys. Rev. A **67**, 015601 (2003).
[9] L. M. Pismen, *Vortices in Nonlinear Fields* (Clarendon Press, Oxford, 1999).
[10] E. Lundh and P. Ao, Phys. Rev. A **61**, 063612 (2000).
[11] A. L. Fetter and A. A. Svidzinsky, J. Phys. Condens. Matter **13**, R135 (2001).
[12] P. Rosenbusch, V. Bretin, and J. Dalibard, Phys. Rev. Lett. **89**, 200403 (2002).
[13] J. J. Garcia-Ripoll and V. M. Perez-Garcia, Phys. Rev. A **63**, 041603 (2001).
[14] T. Busch and J. R. Anglin, Phys. Rev. Lett. **84**, 2298 (1999).
[15] N. G. Parker, N. P. Proukakis, M. Leadbeater, and C. S. Adams, Phys. Rev. Lett. **90**, 220401 (2003).
[16] A. Görlitz *et al.*, Phys. Rev. Lett. **87**, 130402 (2001).
[17] D. Rychtarik, B. Engeser, H. C. Nagerl, and R. Grimm, cond-mat/0309536 [Phys. Rev. Lett. (to be published)].
[18] D. S. Petrov, M. Holzmann, and G. V. Shlyapnikov, Phys. Rev. Lett. **84**, 2551 (2000).
[19] U. Al Khawaja, J. O. Anderson, N. P. Proukakis, and H. T. C. Stoof, Phys. Rev. A **66**, 013615 (2002).
[20] B. P. Anderson, P. C. Haljan, C. E. Wieman, and E. A. Cornell, Phys. Rev. Lett. **85**, 2857 (2000).
[21] B. Jackson, J. F. McCann, and C. S. Adams, Phys. Rev. A **61**, 013604 (2000).
[22] A. A. Svidzinsky and A. L. Fetter, Phys. Rev. A **62**, 063617 (2000).
[23] M. D. Lee, S. A. Morgan, M. J. Davis, and K. Burnett, Phys. Rev. A **65**, 043617 (2002).
[24] B. M. Caradoc-Davies, R. J. Ballagh, and K. Burnett, Phys. Rev. Lett. **83**, 895 (1999).
[25] P. G. Kevrekidis *et al.*, J. Phys. B **36**, 3467 (2003).
[26] See I. Biktasheva and V. N. Biktashev, Phys. Rev. E **67**, 026221 (2003), and references therein.
[27] D. P. Arovas and J. A. Friere, Phys. Rev. B **55**, 1068 (1997), and references therein.
[28] D. Rozas, Z. S. Sacks, and G. A. Swartlander, Jr., Phys. Rev. Lett. **79**, 3399 (1997).